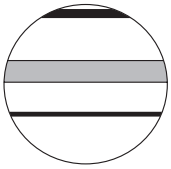

Research report

COMNISPA II: Update of a mid-European isotope climate record, 11 ka to present

The Holocene
23(5) 749–754

DOI: 10.1177/0959683612465446
hol.sagepub.com

Jens Fohlmeister,[1] Nicole Vollweiler,[1,2] Christoph Spötl[3] and Augusto Mangini[1]

Abstract

We present an update (COMNISPA II) of a precisely dated, high-resolution speleothem $\delta^{18}O$ record from the Austrian Alps. COMNISPA II consists of five stalagmites from Spannagel Cave, which have comparable $\delta^{18}O$ values within periods of simultaneous growth and show similar $\delta^{18}O$ variations on centennial to millennial timescales. This allows combining the five stalagmites to one composite record using a newly developed statistical approach. The COMNISPA II stack differs slightly from the previous version, but is better constrained because of additional stalagmites used for the reconstruction and a more objective method used for constructing the composite record. Furthermore, the record now covers the last 11 ka and shows variations in $\delta^{18}O$ values by about 2‰. As previously shown, these variations compare well with other records in central Europe and the North Atlantic, and thus reflect a large-scale climate evolution.

Keywords

climate, Holocene, oxygen isotopes, speleothem

Received 26 March 2012; revised manuscript accepted 28 September 2012

Introduction

Understanding natural climate variability on different timescales is an important key to predict future climate change. Especially the Holocene offers great potential to investigate climate anomalies during a rather stable interglacial. In the recent past speleothems have become important climate archives as they record climate variability (preferentially in their O isotope composition), often even at high (i.e. decadal to annual) resolution, and can be radiometrically dated by U-series methods (for reviews see Fairchild et al., 2006; Lachniet, 2009; McDermott, 2004). Recent theoretical studies of O isotopes in the soil and karst system (Baker and Bradley, 2010; Bradley et al., 2010; Wackerbarth et al., 2010) and of the detailed mechanisms of calcite deposition (Dreybrodt and Scholz, 2011; Mühlinghaus et al., 2009; Scholz et al., 2009) show that the climate signal of meteoric precipitation and/or temperature is well captured in speleothems. These findings are supported by many field studies which reveal a relationship between the $\delta^{18}O$ record and climate parameters (Jex et al., 2010; Lachniet et al, 2004; Lauritzen and Lundberg, 1999; Mangini et al., 2005).

Proxy signals in individual stalagmites, however, do not necessarily reflect climate, but can be influenced by local differences in e.g. soil cover, seepage hydrology and cave ventilation regimes (cf. Fairchild and Baker, 2012, for an up-to-date review). Replication by sampling multiple stalagmites of comparable growth morphology within a given cave is therefore essential to validate proxy time series (Dorale et al., 1998; Spötl et al., 2006; Vollweiler et al., 2006; Wang et al., 2001). Typically, data from two or more stalagmites are combined to a composite record (Spötl et al., 2006; Vollweiler et al., 2006; Zhao et al., 2010). The procedure of combining individual records is often guided by more or less subjective decisions. This might explain why the potential to improve age–depth models by the use of additional information provided by several simultaneously grown stalagmites has rarely been explored. COMNISPA is an example of a combined stable isotope record (Vollweiler et al., 2006) used for interpreting Holocene climate variability (Mangini et al., 2007). This record is based on three stalagmites (SPA 12, 128 and 70) from Spannagel Cave (Austria) characterized by clean, U-rich calcite giving rise to precise U/Th chronologies. Stalagmite SPA 12 covers the period AD 1950 back to about 5 ka (NB: all U/Th ages, unless otherwise noted, refer to the year AD 2004). Its age model is constrained by 13 U/Th ages. Eleven ages were used for the age–depth model construction of SPA 128 covering the period between 2.5 and 4.6 ka. SPA 70 contributed data between 5 and 8.8 ka, which was constrained by eight dates. The oldest part of the stalagmite SPA 128 was not used in COMNISPA, because the age model was compromised by a possible hiatus. Also the youngest part of SPA 70 (<5 ka) suffered from a possible hiatus and was discarded in the former study.

Here we provide an update, COMNISPA II, which (a) is based on five stalagmites from the same cave, (b) extends the record back to 11 ka and (c) employs a new statistical procedure (*iscam*; Fohlmeister, 2012) to produce a stack using improved age–depth models including error estimates.

[1]Heidelberg Academy of Sciences, Germany
[2]Heidelberg Center for the Environment (HCE), Germany
[3]Institute for Geology und Paleontology, University of Innsbruck, Austria

Corresponding author:
Jens Fohlmeister, Heidelberg Academy of Sciences, Im Neuenheimer Feld 229, 69120 Heidelberg, Germany.
Email: jens.fohlmeister@iup.uni-heidelberg.de

Cave site

Spannagel Cave is situated in the rear of the Tux Valley (Zillertal Alps, western Austria). The cave stretches some 11 km from 2524 down to 2198 m a.s.l. and developed in a contact karst setting. During most glacials and during some periods of the Holocene large parts of the cave were covered by the nearby temperate Tux glacier. Ice coverage does not necessarily mean that stalagmite growth stopped as shown by replicated intervals of slow calcite deposition during stadials (Spötl et al., 2006). During these subglacial conditions marble dissolution was fuelled by acidity generated by the oxidation of disseminated sulfide minerals in the marble and the overlying gneiss (Spötl and Mangini, 2007) and speleothem deposition was confined to passages unaffected by flooding during the summer ablation period. In warm, interglacial climates sparse alpine soils developed on the ice-free landscape above the cave giving rise to an additional pedogenic source of acidity. This interplay between the two processes is reflected by e.g. the highly variable C isotope values in Spannagel speleothems. In contrast, the O isotopic composition represents a direct atmospheric proxy, i.e. of precipitation above the cave. Given that today's cave temperature is barely above the freezing point and calcite deposition was continuous even during the 'Little Ice Age' (Mangini et al., 2005) temperature changes inside the cave during the Holocene were likely small; hence, the $\delta^{18}O$ signal of the calcite largely reflects atmospheric $\delta^{18}O$ changes.

All five stalagmites were found in situ in the eastern part of the cave system, which was never ice-covered during the Holocene. In contrast, the western branches of the cave were repeatedly underneath the ice of the Tux Glacier (e.g. Spötl and Mangini, 2010). In addition to stalagmites SPA 12, 70 and 128 which were used in the first version of COMNISPA, we sampled SPA 127 and 133 (Figure 1). Four stalagmites grew within 74 m inside the Tropfsteingang gallery and SPA 127 was found in the Blockhalle chamber 140 m away. The sampling sites Tropfsteingang and Blockhalle are at an elevation of 2310 and 2340 m a.s.l., and the cave air temperature today is 2.0 ±0.1 and 1.7 ±0.1°C, respectively.

Methods

The two new stalagmites SPA 127 and 133 were dated in the same laboratory and using identical protocols as the three previous stalagmites. We also performed additional U/Th age measurements to improve the published age models of SPA 12, 70 and 128. U/Th measurements were performed on a thermal ionization mass spectrometer (Finnigan MAT 262 RPQ) with a double filament technique at the Heidelberg Academy of Sciences. Detritial correction using a $^{232}Th/^{238}U$ mass ratio of 3.8 (Wedepohl, 1995) led to negligible age changes because of the very low ^{232}Th concentrations. All ages were calculated using half lives of 75,381 yr for ^{230}Th, 244,600 yr for ^{234}U, and 4.4683×10^9 yr for ^{238}U (Cheng et al., 2000). The quoted age uncertainties do not include the half-life uncertainties. All ages refer to AD 2004, the year of the measurements for the stalagmites included in the first version of COMNISPA (Table 1). Typical age errors are smaller than 2%.

Samples for oxygen isotope analysis of SPA 127 and 133 were micromilled at 100 µm increments and measured using an online, automated carbonate preparation system linked to a triple collector gas source mass spectrometer at the University of Innsbruck. Values are reported relative to the Vienna Pee Dee Belemnite standard. The long-term precision of the $\delta^{18}O$ values (1σ standard deviation of replicate analyses) is 0.08% (Spötl, 2011; Spötl and Vennemann, 2003). The statistical properties of the $\delta^{18}O$ measurements of the individual stalagmites are listed in Table 2.

Construction of the COMNISPA II stack

We constructed a composite record of the five stalagmite proxy records which overlap temporally (Figure 2). We use *iscam* (Fohlmeister, 2012) which is based on Monte-Carlo (MC) age

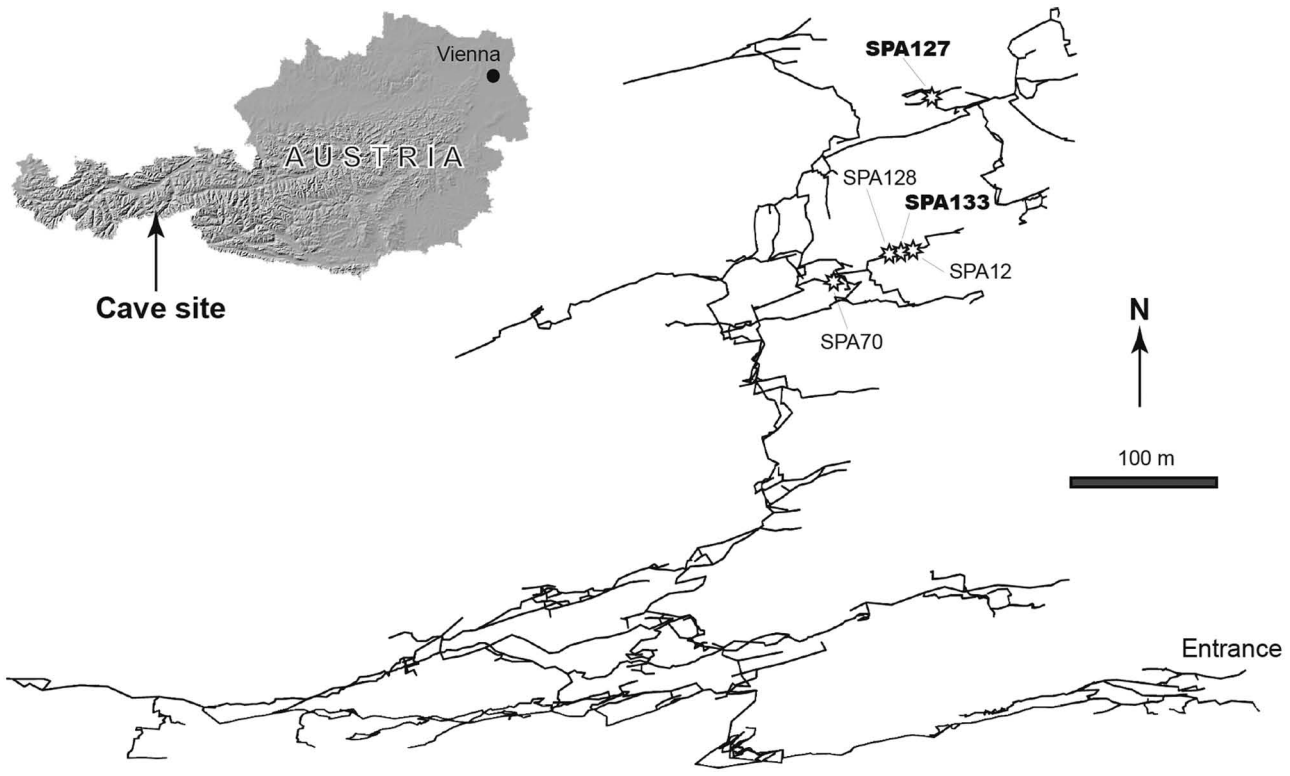

Figure 1. Plan view of Spannagel Cave in western Austria showing the locations of the additional two stalagmites (bold labels) on which COMNISPA II is based in addition to the three stalagmites which were already part of the previous version of COMNISPA.

Table 1. Results of U-series measurements. Samples marked by an asterisk were already published in Vollweiler et al. (2006). Ages represent detritus-corrected values and refer to AD 2004. Errors depict 2-σ uncertainties.

Sample	Distance from top (cm)	δU (‰)	Error	^{238}U (ppm)	Error	^{230}Th (pg/g)	Error	^{230}Th/^{232}Th ($\times 10^{-6}$)	Error	Corrected age (ka)	Error
SPA 12(0.2)*	0.2±0.2	16.3	2.9	10.798	0.022	0.1136	0.0068	48	3	0.06	0.004
SPA 12(1.5)*	1.5±0.2	27.8	4.6	13.863	0.035	0.4914	0.0108	854	19	0.23	0.005
SPA 12(3.4)*	3.4±0.2	16.1	2.8	13.635	0.026	0.7929	0.0151	697	14	0.382	0.008
SPA 12(4.8)*	4.8±0.1	13.7	1.4	13.669	0.014	1.1388	0.0239	1251	28	0.548	0.012
SPA 12(6.0)*	6.0±0.1	14.1	1.5	8.827	0.009	1.0128	0.0182	519	10	0.751	0.014
SPA 12(8.0)*	8.0±0.2	25.5	2.9	10.18	0.022	1.8463	0.0517	2430	220	1.179	0.033
SPA 12(10.0)*	10.0±0.2	14	7.7	10.187	0.014	2.1676	0.1	427	13	1.401	0.064
SPA 12(12.0)*	12.0±0.2	22.2	3	10.891	0.025	2.9204	0.073	1537	126	1.749	0.044
SPA 12(13.2)	13.2±0.2	15.6	1.7	11.226	0.011	3.3362	0.0434	333	9	1.967	0.026
SPA 12(14.2)	14.2±0.2	13.1	1.7	10.563	0.011	3.363	0.047	2861	42	2.109	0.03
SPA 12(14.7)*	14.7±0.2	24.5	3.3	11.325	0.026	3.6995	0.0407	1140	17	2.154	0.026
SPA 12(14.8)	14.8±0.2	17.2	1.7	11.979	0.012	4.0243	0.0402	2536	29	2.219	0.023
SPA 12(15.1)	15.1±0.1	14.9	1.9	12.373	0.012	4.125	0.099	1408	16	2.207	0.053
SPA 12(16.6)*	16.6±0.2	11	6.5	8.407	0.019	4.2738	0.0596	1292	33	3.392	0.05
SPA 12(18.0)*	18.0±0.2	4.9	6.9	6.922	0.008	4.4572	0.0525	n.d.	n.d.	4.348	0.06
SPA 12(20.3)*	20.3±0.2	8.7	6.8	10.852	0.016	8.145	0.1414	28191	6603	5.043	0.09
SPA 128(0.3)*	0.3±0.2	15.6	1.6	12.653	0.013	4.845	0.073	442	7	2.52	0.039
SPA 128(1.0)*	1.0±0.2	18.2	1.4	13.199	0.013	5.361	0.059	126	1	2.603	0.03
SPA 128(1.6)*	1.6±0.2	15.3	1.4	12.108	0.012	4.973	0.07	385	6	2.703	0.039
SPA 128(2.6)*	2.6±0.2	10.1	1.2	13.433	0.013	5.912	0.077	445	6	2.918	0.038
SPA 128(3.4)*	3.4±0.2	14.6	1.3	13.513	0.014	6.397	0.041	441	3	3.128	0.021
SPA 128(4.4)*	4.4±0.2	16.1	1.4	13.671	0.014	6.61	0.059	553	5	3.197	0.03
SPA 128(5.5)*	5.5±0.2	14.1	1.3	13.491	0.013	7.222	0.072	246	3	3.518	0.036
SPA 128(6.5)*	6.5±0.2	16.2	1.6	13.662	0.014	8.234	0.206	275	7	3.968	0.102
SPA 128(6.9)*	6.9±0.2	13	1.4	11.787	0.012	7.338	0.081	102	1	4.006	0.045
SPA 128(7.6)*	7.6±0.2	16.3	2.1	11.893	0.012	7.687	0.092	281	4	4.263	0.053
SPA 128(8.5)*	8.5±0.2	13.7	1.3	11.49	0.011	7.979	0.065	399	4	4.62	0.04
SPA 128(8.7)	8.7±0.2	9.8	1.9	10.88	0.011	7.879	0.074	645	7	4.861	0.047
SPA 128(9.2)	9.2±0.2	10.8	1.7	12.699	0.013	9.465	0.114	699	9	5.003	0.063
SPA 128(9.5)*	9.5±0.2	15.5	1.4	11.319	0.011	9.224	0.129	1072	16	5.468	0.08
SPA 128(10.3)	10.3±0.1	7.4	1.7	12.275	0.012	10.736	0.069	599	4	5.91	0.041
SPA 128(10.7)*	10.7±0.2	7.4	1.9	9.502	0.01	8.64	0.15	465	8	6.14	0.11
SPA 70(6.1)	6.1±0.2	20.9	1.5	6.494	0.007	4.434	0.027	2978	20	4.549	0.03
SPA 70(6.5)	6.5±0.2	14.7	1.7	7.353	0.007	5.064	0.066	6168	88	4.621	0.063
SPA 70(7.3)*	7.3±0.2	19.5	2.7	6.747	0.013	5.143	0.077	1869	30	5.094	0.079
SPA 70(8.6)*	8.6±0.2	21.3	2.7	11.39	0.016	10.098	0.095	6181	62	5.946	0.061
SPA 70(11.6)*	11.6±0.2	13.5	1.5	16.604	0.017	15.34	0.11	9318	68	6.254	0.046
SPA 70(14.0)*	14.0±0.2	10.7	2.3	23.348	0.035	24.32	0.14	3311	21	7.092	0.046
SPA 70(16.0)*	16.0±0.1	5.9	1.6	28.758	0.029	32.47	0.15	2023	11	7.743	0.039
SPA 70(17.3)*	17.3±0.2	8.2	4.7	40.861	0.118	49.12	0.34	9813	82	8.256	0.076
SPA 70(18.0)*	18.0±0.1	6.2	2.2	33.582	0.057	41.67	0.33	4413	37	8.546	0.072
SPA 70(18.5)*	18.5±0.1	3	1.4	28.646	0.029	36.66	0.23	1035	7	8.828	0.058
SPA 70(19.5)*	19.5±0.2	−4.1	2.6	45.767	0.092	64.69	0.25	3355	16	9.894	0.052
SPA 127(0.5)	0.5±0.1	27	1.6	5.3757	0.0054	2.237	0.074	n.d.	n.d.	2.737	0.09
SPA 127(3.65)	3.65±0.2	11.3	1.4	5.1292	0.0051	3.376	0.074	16741	405	4.429	0.1
SPA 127(4.5)	4.5±0.1	8.2	2.1	6.2974	0.0063	4.431	0.177	13488	597	4.757	0.198
SPA 127(5.1)	5.1±0.1	4.3	1.7	6.749	0.0067	5.124	0.102	44193	1031	5.164	0.106
SPA 127(6.0)	6.0±0.1	−5.5	1.4	7.6523	0.0077	6.558	0.043	62061	455	5.906	0.041
SPA 127(8.5)	8.5±0.1	−4.3	1.6	9.4671	0.0095	9.308	0.082	28352	274	6.795	0.063
SPA 127(11.0)	11.0±0.1	3.2	1.4	13.98	0.014	15.723	0.157	116447	1383	7.749	0.082
SPA 127(12.5)	12.5±0.1	1.6	1.4	25.236	0.028	29.315	0.185	78831	664	8.026	0.055
SPA 127(14.5)	14.5±0.1	−7.2	1.4	34.374	0.034	41.579	0.457	106273	1415	8.449	0.101
SPA133(6.5)	0.65±0.2	−5.5	1.8	65.894	0.066	93.69	0.52	n.d.	n.d.	9.983	0.061
SPA133(12.5)	1.25±0.2	−5.6	1.4	70.884	0.071	103.37	0.93	n.d.	n.d.	10.253	0.098
SPA133(21.5)	2.15±0.2	−6.7	1.4	97.441	0.097	142.2	1.2	n.d.	n.d.	10.268	0.092
SPA133(32.0)	3.2±0.2	−11.6	1.4	109.04	0.11	159.8	1.2	n.d.	n.d.	10.371	0.085
SPA133(43.0)	4.3±0.2	−7.8	1.4	102.84	0.1	153.78	0.88	n.d.	n.d.	10.55	0.066
SPA133(53.0)	5.3±0.2	−6.1	1.4	93.755	0.094	142.2	1.1	n.d.	n.d.	10.691	0.089
SPA133(66.5)	6.65±0.2	−2.9	1.4	68.673	0.069	105.63	0.45	n.d.	n.d.	10.811	0.053

Table 2. Statistical properties of the five speleothem $\delta^{18}O$ records. Note that the mean $\delta^{18}O$ value of the individual stalagmites is not an indicator for the shift used to build the composite record. Instead, the shift is calculated from the $\delta^{18}O$ values of coeval parts of the individual stalagmites.

	SPA 12	SPA 128	SPA 70	SPA 127	SPA 133
Number of measurements	1070	1060	684	1530	713
Mean $\delta^{18}O$	−7.55‰	−8.01‰	−8.39‰	−8.22‰	−7.94‰
Std $\delta^{18}O$	0.29‰	0.28‰	0.3‰	0.35‰	0.42‰
Min $\delta^{18}O$	−8.58‰	−9.18‰	−9.41‰	−9.94‰	−8.87‰
Max $\delta^{18}O$	−6.76‰	−7.19‰	−7.71‰	−7.42‰	−6.76‰
Average resolution	5.1 yr	3.5 yr	8 yr	4 yr	1.6 yr
Time range	AD 1963–5.5 ka	2.5–6.1 ka	4.5–10 ka	2.6–8.5 ka	9.7–10.8 ka
$\delta^{18}O$ shift for composite record	–[a]	0.42‰	0.38‰	0.36‰	–[b]

Notes: [a]SPA12 is the reference stalagmite and was thus not shifted for the composite record.
[b]SPA 133 was not shifted, because of the minimal temporal overlap with the other stalagmites (section Construction of the COMNISPA II stack).

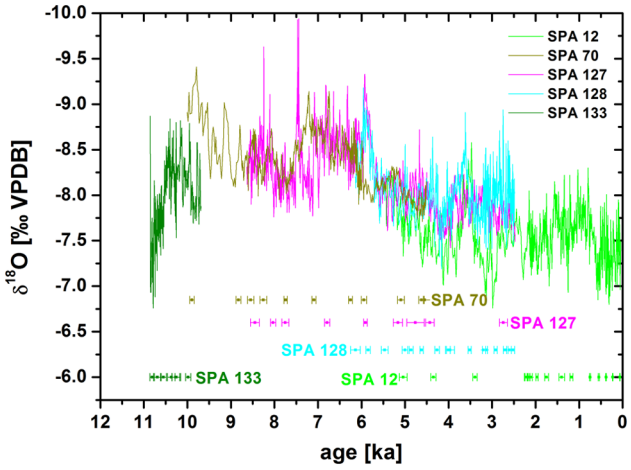

Figure 2. Untuned $\delta^{18}O$ time series of the five Spannagel stalagmites. The age control points (including their analytical uncertainties) of the five stalagmites are shown in the lower part of the diagram.

simulations and correlation calculations between pairs of climate records. The advantage of this approach is that the age–depth models of the individual records benefit from the information provided by the other synchronously grown stalagmites by correlating $\delta^{18}O$ values, which generally show similar patterns in stalagmites from one cave. Hence the age models can be improved and the age uncertainties can be reduced. Finally, *iscam* constructs a composite record, which is mainly determined by the best correlations. The software provides an objective estimate of the 'best' age–depth model using all available data. Free parameters in *iscam* include (a) the way of interpolation between dated depths, (b) the degree of smoothing during correlation calculations, and (c) prior detrending and the normalisation of the time series.

In the overlapping period of two stalagmites *iscam* randomly varies the measured ages within their analytical age errors. We added a few lines of code to *iscam* to allow depth variations within the drill width of the individual subsamples. We prescribed a point-wise linear interpolation between data points. The resulting age–depth models were then applied to the $\delta^{18}O$ data of the five stalagmites. Note that this approach differs from the depth–age relationship on which the first version of COMNISPA was based (i.e. Akima-spline interpolation between individual data points; Vollweiler et al., 2006). The best correlation between two $\delta^{18}O$ time series is defined as the 'best' age–depth model. A composite record of the first two stalagmites is established by shifting the $\delta^{18}O$ level of the second stalagmite to the level of the first one and averaging both signals. This procedure is then applied to the previously combined two records and a third one. In the case of the Spannagel stalagmites this procedure was performed three times. For each step, the 'best' age–depth model was found from 100,000 MC simulations. The significance estimation for the several steps was performed using 2000 pairs of artificially constructed first-order autoregressive time series (AR1). Each pair of the 2000 AR1 processes was scanned with 1000 MC simulations to find the best correlation.

The resulting composite record covers the period between 10 ka and AD 1963 (Figure 3). At least two stalagmites grew contemporaneously between 8.5 and 2.5 ka. Outside the overlapping interval a simple point-wise linear interpolation between dated points was applied. Therefore, for the last approximately 2.5 ka COMNISPA II is similar to the initial COMNISPA record (Vollweiler et al., 2006). SPA 133 only shows a very short temporal overlap with the other stalagmites. The youngest age of SPA 133 is approximately 100 yr older than the oldest measured age of SPA 70. The age–depth relationship for $\delta^{18}O$ suggests that both records overlap by a maximum of 100 yr. Owing to this small overlap, we did not use SPA 133 for the construction of the stacked record. However, we used the $\delta^{18}O$ data of SPA 133 to provide an idea of the O isotope values during the onset of the Holocene. In other words, this stalagmite is only attached to the composite record consisting of SPA 12, 127, 128 and 70. However, we emphasize that all five stalagmites from Spannagel Cave are part of COMNISPA II.

Discussion

Comparison with the previous version

The first version of COMNISPA consisted of three stalagmites (SPA 12, 128 and 70) combined in a composite record. Then, possible hiati and corresponding age-model uncertainty limited the use of SPA 70 and 128. Therefore, isotope data of SPA 70 younger than 4.6 ka were not used. In addition, isotope measurements of SPA 128 older than 4.6 ka were discarded for the same reason. In order to combine the three stalagmites the offset between SPA 12 and 128 was subtracted from the former and the mean of both $\delta^{18}O$ curves was calculated for the overlapping period. SPA 70 was adjusted to the combined curve in the same manner.

For COMNISPA II additional ages were measured for the three stalagmites (Table 1). Especially in the old part of SPA 128 (between 6.1 and 4.6 ka) the age model was refined, resulting in a reliable age–depth relationship from the entire stalagmite. Unfortunately the additional U-series measurements in the upper part of SPA 70 did not solve the question of a possible hiatus between 4.6 and 3.6 ka. Therefore this part of SPA 70 is not included in COMNISPA II. This period, however, is now covered by SPA 127, one of the two new specimens included in the stack. This stalagmite grew from about 8.45 to 2.24 ka and provides additional support of the signal recorded by SPA 70, since in periods of

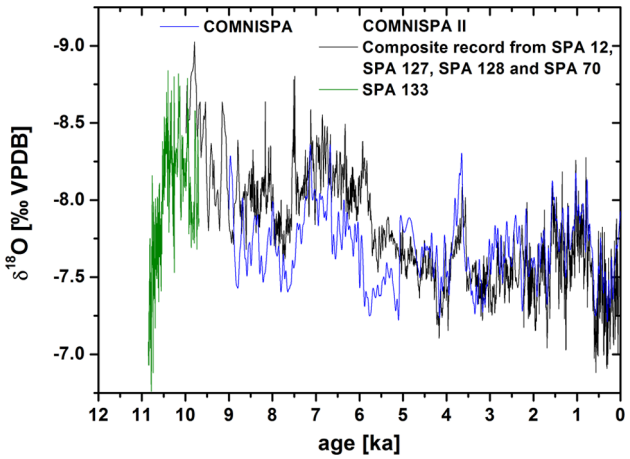

Figure 3. Comparison of the first COMNISPA (blue) version with COMNISPA II: stalagmites SPA 12, 127, 128 and 70 where used to construct the $\delta^{18}O$ composite record (black) for the last 10 ka. This data set is complemented by SPA 133 (green), which grew between 11 and 10 ka. It was not possible to connect SPA 133 with the remaining record, because the overlap is too short. Therefore, we prefer to show the data of SPA 133 on its original $\delta^{18}O$ level as a single record and refrain from combining SPA 133 with the other stalagmite time series. Nevertheless, SPA 133 is part of the COMNISPA II record and shows the evolution and variability of $\delta^{18}O$ near the onset of the Holocene.

contemporaneous growth (between 8.45 and 4.55 ka) both show consistent $\delta^{18}O$ patterns.

Both versions of COMNISPA are similar for approximately the last 2.5 ka. Before 2.5 ka COMNISPA II is slightly different from its previous version, since this new stack is composed of three stalagmites in this period. Also the new procedure applied to produce the stacked age model improved the age–depth relationship considerably. The $\delta^{18}O$ anomaly between 3.9 and 3.5 ka is now smoother, because the signal is not as pronounced in SPA 127 as in SPA 12 and 128. The additional stalagmite and the different age-model approach result in a shift of the end of this event by about 70 yr towards younger ages. The large O isotope anomaly between about 5.2 and 4.8 ka of the first version is not present in COMNISPA II. This period was largely affected by the method of stack construction, i.e. SPA 70 was 'glued' to the starting point of SPA 12 after subtracting the offset between both $\delta^{18}O$ series. This in combination with an overestimated offset between SPA 70 and 12 had resulted in the $\delta^{18}O$ anomaly which disappeared in COMNISPA II. With the new age modelling approach and the newly available stalagmite SPA 127 the $\delta^{18}O$ signal does not show large variations at this time. Instead, there is now a rather gradual increase in the $\delta^{18}O$ values. Before 5 ka COMNISPA II values are about 0.4 to 0.5‰ lower than in the previous record, which is ascribed to the smaller offset subtracted from the $\delta^{18}O$ data of SPA 70 and 127 compared with the first version of COMNISPA. Furthermore, the new age model suggests slightly different ages than before. Between 7 and 5 ka COMNISPA II is younger than the first version (about 330 yr around 6.5 ka and about 210 yr at around 5.8 ka). Two effects explain this shift. First, we now have additional age constraints from the early part of SPA 128 and from SPA 127. In addition SPA 127 and SPA 128 show the decrease in $\delta^{18}O$ some 100 years later than SPA 70 (Figure 2). COMNISPA II suggests up to about 180 yr older ages between 9 to 7 ka because of additional age constraints provided by SPA 127. The new stalagmite SPA 133 extends the overall record further back in time by about 2 kyr.

Climate interpretation

In contrast to minor changes in the stack, the interpretation of the $\delta^{18}O$ record with respect to climate has remained unchanged. Owing to the low cave temperature kinetic isotope effects are minimal (Mangini et al., 2005; Vollweiler et al., 2006). The short-term variations in COMNISPA II are in response to temperature, whereas for the late Holocene (the last 2 ka) Mangini et al. (2005) provided a transfer function between stalagmite $\delta^{18}O$ values and air temperature. They showed that for Spannagel cave higher $\delta^{18}O$ values characterize a colder climate and vice versa. The relationship between temperature and $\delta^{18}O$ at Spannagel Cave is explained by two alternative mechanisms. Either the relationship results from variable contributions of summer versus winter precipitation to the karst reservoir feeding the drip sites. This change in precipitation pattern, especially in winter, is closely related to temperature changes (Wackerbarth et al., 2010). Another mechanism discussed by Mangini et al. (2005) are changes in the strength of the North Atlantic Oscillation (NAO) which might be reflected in the $\delta^{18}O$ values of the stalagmites. This is supported by instrumental observations in central Europe between the strength of the winter NAO+ situations, accompanied by higher-than-average temperatures, and the $\delta^{18}O$ of winter precipitation (Baldini et al., 2008). The proposed relationship between $\delta^{18}O$ and temperature might not be valid for the entire Holocene. During the Younger Dryas and the transition into the early Holocene atmospheric circulation pattern might have been sufficiently different from the present-day situation and thus, prohibit the use of the T–$\delta^{18}O$ relationship established for the late Holocene. The observed strong decrease in the $\delta^{18}O$ by about 1.5‰ between 11 and 10 ka, for example, is rather a change of the source region than a pure temperature effect. Based on this assumption, during the deglaciation the trajectories more frequently followed southerly routes. Towards the transition into the Holocene the main contribution of precipitation probably originated from more northern regions of the Atlantic, where the surface ocean is generally more depleted in ^{18}O (LeGrande and Schmidt, 2006).

The trend of increasing $\delta^{18}O$ during the Holocene is consistent with temporal changes in the isotope gradients recorded by combining results from low-elevation European speleothem sites (McDermott et al., 2011). However, the temporal change in $\delta^{18}O$ observed in the COMNISPA II record is considerably greater than that predicted for this latitude using McDermott's isotope gradient. Especially at around 6 ka COMNISPA II records a strong shift in the $\delta^{18}O$ levels from lower values in the early and mid Holocene to higher values in the late Holocene. The larger change in $\delta^{18}O$ and the relative abrupt shift at 6 ka possibly reflect an enhanced rainout trend during the Holocene at high-elevation sites.

Several studies have shown that the COMNISPA record is representative of the Alpine climate (Grosjean et al., 2007; Hormes et al., 2008;Vollweiler et al., 2006). However, other studies also showed that the observed O signal of this site followed large-scale climate variations. Spannagel $\delta^{18}O$ records and growth phases are in agreement with the $\delta^{18}O$ pattern in Greenland ice cores on millennial to orbital timescales (Spötl and Mangini, 2007 Spötl et al., 2006), with sediment proxies and growth of deep-sea corals from the North Atlantic (Frank et al., 2009; Mangini et al., 2005) and with other stalagmites from central Europe (Mangini et al., 2007). Trouet et al. (2009) found and discussed similarities of Spannagel speleothem $\delta^{18}O$ values in relation to their NAO reconstruction for the past 1000 yr based on speleothem data from Scotland (Proctor et al., 2000) and tree-ring data from Morocco (Esper et al., 2007). In addition, the super-regional character of our alpine location was explicitly demonstrated in a proxy intercomparison study investigating teleconnections between the tropical Pacific and mid-latitude regions (Graham et al., 2007).

Conclusion

We updated the COMNISPA stalagmite record by improving the chronology of the three existing stalagmites SPA 12, 70 and 128 and by adding two new specimens, SPA 127 and 133. During periods of simultaneous growth the individual stalagmites show the same overall $\delta^{18}O$ pattern. This enabled us to apply an improved stacking procedure to splice these isotope records together. The resulting composite record, COMNISPA II, covers almost the entire Holocene, i.e. the last 11 ka. The oldest record (SPA 133) shows only a very short overlap and was therefore only attached to the composite record of the remaining four stalagmites. Between 8.5 and 2.5 ka the stack consists of at least two stalagmites. Apart from extending the record back to 11 ka the most important changes in COMNISPA II are small adjustments of about ± 180 yr between 9 ka and 5 ka because of the use of a second stalagmite covering large parts of this interval providing more constraints on the final age model. An O isotope anomaly at about 5 ka vanished and is replaced by a gradual increase in $\delta^{18}O$ values.

Acknowledgements

The authors are grateful to two journal referees for their helpful comments.

Funding

JF and NV received funding from the German Research Foundation (FG 668 and MA 821/36-1). CS acknowledges funding by FWF.

References

Baker A and Bradley C (2010) Modern stalagmite $\delta^{18}O$: Instrumental calibration and forward modelling. *Global and Planetary Change* 71: 201–206.

Baldini LM, McDermott F, Foley AM et al. (2008) Spatial variability in the European winter precipitation $\delta^{18}O$–NAO relationship: Implications for reconstructing NAO-mode climate variability in the Holocene, *Geophysical Research Letters* 35: L04709, doi:10.1029/2007GL032027.

Bradley C, Baker A, Jex CN et al. (2010) Hydrological uncertainties in the modelling of cave drip-water $\delta^{18}O$ and the implications for stalagmite palaeoclimate reconstructions. *Quaternary Science Reviews* 29: 2201–2214.

Cheng H, Edwards RL, Hoff J et al. (2000) The half-lives of uranium-234 and thorium-230. *Chemical Geology* 169: 17–33.

Dorale JA, Edward RL, Ito E et al. (1998) Climate and vegetation history of the midcontinent from 75 to 25 ka: A speleothem record from Crevice Cave, Missouri, USA. *Science* 282: 1871–1874.

Dreybrodt W and Scholz D (2011) Climatic dependence of stable carbon and oxygen isotope signals recorded in speleothems: From soil water to speleothem calcite, *Geochimica et Cosmochimica Acta* 75: 734–752.

Esper J, Frank D, Büntgen U et al. (2007) Long-term drought severity variations in Morocco. *Geophysical Research Letters* 34: L17702, doi:10.1029/2007GL030844.

Fairchild IJ and Baker A (2012) *Speleothem Science: From Process to Past Environments*. Wiley-Blackwell.

Fairchild IJ, Smith CL, Baker A et al. (2006) Modification and preservation of environmental signals in speleothems. *Earth Science Reviews* 75: 105–153.

Fohlmeister J (2012) A statistical approach to construct composite climate records of dated archives. *Quaternary Geochronology* http://dx.doi.org/10.1016/j.quageo.2012.06.007

Frank N, Ricard E, Lutringer-Paquet A et al. (2009) The Holocene occurrence of cold water corals in the NE Atlantic: Implications for coral carbonate mound evolution. *Marine Geology* 266: 129–142.

Graham NE, Hughes MK, Ammann CM et al. (2007) Tropical Pacific–mid-latitude teleconnections in medieval times. *Climatic Change* 83: 241–285.

Grosjean M, Suter PJ, Trachsel M et al. (2007) Ice-borne prehistoric finds in the Swiss Alps reflect Holocene glacier fluctuations. *Journal of Quaternary Science* 22: 203–207.

Hormes A, Ivy-Ochs S, Kubik PW et al. (2008) ^{10}Be exposure ages of a rock avalanche and a late glacial moraine in Alta Valtellina, Italian Alps. *Quaternary International* 190: 136–145.

Jex CN, Baker A, Fairchild IJ et al. (2010) Calibration of speleothem $\delta^{18}O$ with instrumental climate records from Turkey. *Global and Planetary Change* 71: 207–217.

Lachniet MS (2009) Climatic and environmental controls on speleothem oxygen-isotope values. *Quaternary Science Reviews* 28: 412–432.

Lachniet MS, Burns SJ, Piperno DR et al. (2004) A 1500-year El Nino/Southern Oscillation and rainfall history for the Isthmus of Panama from speleothem calcite. *Journal of Geophysical Research* 109: D20117, doi: 10.1029/2004JD004694.

Lauritzen SE and Lundberg J (1999) Calibration of the speleothem delta function: An absolute temperature record for the Holocene in northern Norway. *The Holocene* 9: 659–669.

LeGrande AN and Schmidt GA (2006) Global gridded data set of the oxygen isotopic composition in seawater. *Geophysical Research Letters* 33: L12604, doi:10.1029/2006GL026011.

McDermott F (2004) Palaeo-climate reconstruction from stable isotope variations in speleothems: A review. *Quaternary Science Reviews* 23: 901–918.

McDermott F, Atkinson TC, Fairchild IJ et al. (2011) A first evaluation of the spatial gradients in $\delta^{18}O$ recorded by European Holocene speleothems. *Global and Planetary Change* 79: 275–287.

Mangini A, Spötl C and Verdes P (2005) Reconstruction of temperature in the Central Alps during the past 2000 yr from a $\delta^{18}O$ stalagmite record. *Earth and Planetary Science Letters* 235: 741–751.

Mangini A, Verdes P, Spötl C et al. (2007) Persistent influence of the North Atlantic hydrography on Central European winter temperature during the last 9000 years. *Geophysical Research Letters* 34: 2704, L02704, doi:10.1029/2006GL028600.

Mühlinghaus C, Scholz D and Mangini A (2009) Modelling fractionation of stable isotopes in stalagmites. *Geochimica et Cosmochimica Acta* 71: 2780–2790.

Proctor CJ, Baker A, Barnes WL et al. (2000) A thousand year speleothem proxy record of North Atlantic climate from Scotland. *Climate Dynamics* 16: 815–820.

Scholz D, Mühlinghaus C and Mangini A (2009) Modelling $\delta^{13}C$ and $\delta^{18}O$ in the solution layer on stalagmite surfaces. *Geochimica et Cosmochimica Acta* 73: 2592–2602.

Spötl C (2011) Long-term performance of the Gasbench isotope ratio mass spectrometry system for the stable isotope analysis of carbonate microsamples. *Rapid Communications in Mass Spectrometry* 25: 1683–1685.

Spötl C and Mangini A (2007) Speleothems and paleoglaciers. *Earth and Planetary Science Letters* 254: 323–331.

Spötl C and Mangini A (2010) Paleohydrology of a high-elevation, glacier influenced karst system in the Central Alps (Austria). *Austrian Journal of Earth Sciences* 103: 92–105.

Spötl C and Vennemann T (2003) Continuous-flow IRMS analysis of carbonate minerals. *Rapid Communications of Mass Spectrometry* 17: 1004–1006.

Spötl C, Mangini A and Richards DA (2006) Chronology and paleoenvironment of Marine Isotope Stage 3 from two high-elevation speleothems, Austrian Alps. *Quaternary Science Reviews* 25: 1127–1136.

Trouet V, Esper J, Graham NE et al. (2009) Persistent positive North Atlantic Oscillation mode dominated the medieval climate anomaly. *Science* 324: 78–80.

Vollweiler N, Scholz D, Mühlinghaus C et al. (2006) A precisely dated climate record for the last 9 kyr from three high alpine stalagmites, Spannagel Cave, Austria. *Geophysical Research Letters* 33: L20703, doi:10.1029/2006GL027662.

Wackerbarth A, Scholz D, Fohlmeister J et al. (2010) Modelling the $\delta^{18}O$ value of cave drip water and speleothem calcite. *Earth and Planetary Science Letters* 299: 387–397.

Wang YJ, Cheng H, Edwards RL et al. (2001) A high-resolution absolute-dated late Pleistocene monsoon record from Hulu Cave, China. *Science* 294: 2345–2348.

Wedepohl HK (1995) The composition of the continental crust. *Geochimica et Cosmochimica Acta* 59: 1217–1232.

Zhao K, Wang Y, Edwards RL et al. (2010) High-resolution stalagmite $\delta^{18}O$ records of Asian monsoon changes in central and southern China spanning the MIS 3/2 transition. *Earth and Planetary Science Letters* 289: 191–198.